

A functionally characterized test set of human induced pluripotent stem cells

Gabriella L Boulting^{1-3,12}, Evangelos Kiskinis^{1,2,12}, Gist F Croft^{4,5,12}, Mackenzie W Amoroso^{4,5,12}, Derek H Oakley^{4,5,12}, Brian J Wainger⁶⁻⁸, Damian J Williams⁹, David J Kahler¹⁰, Mariko Yamaki^{1,2}, Lance Davidow², Christopher T Rodolfa³, John T Dimos^{3,11}, Shravani Mikkilineni^{2,3}, Amy B MacDermott⁹, Clifford J Woolf^{6,7}, Christopher E Henderson^{4,5}, Hynek Wichterle^{4,5} & Kevin Eggan¹⁻³

Human induced pluripotent stem cells (iPSCs) present exciting opportunities for studying development and for *in vitro* disease modeling. However, reported variability in the behavior of iPSCs has called their utility into question. We established a test set of 16 iPSC lines from seven individuals of varying age, sex and health status, and extensively characterized the lines with respect to pluripotency and the ability to terminally differentiate. Under standardized procedures in two independent laboratories, 13 of the iPSC lines gave rise to functional motor neurons with a range of efficiencies similar to that of human embryonic stem cells (ESCs). Although three iPSC lines were resistant to neural differentiation, early neuralization rescued their performance. Therefore, all 16 iPSC lines passed a stringent test of differentiation capacity despite variations in karyotype and in the expression of early pluripotency markers and transgenes. This iPSC and ESC test set is a robust resource for those interested in the basic biology of stem cells and their applications.

Reprogramming of somatic cells to iPSCs presents an opportunity to produce previously inaccessible cell types for disease-related studies¹. iPSCs can be made from patients and their healthy relatives, allowing the genetic variants that either predisposed them to or protected them from disease to be studied²⁻⁵. However, if patient-specific iPSCs are to become a standard resource, it is vital to understand how reliably they generate differentiated derivatives. Among the concerns raised about iPSCs is that reprogramming may be incomplete, resulting in cell lines with variable gene expression or DNA methylation⁶⁻⁸. Indeed, it was reported that when human iPSC lines were differentiated toward a motor neuron identity, they uniformly failed to produce this neural subtype with the efficiency observed using ESCs⁹. Moreover, it has been suggested that differentiated progeny of iPSCs that harbor reprogramming proviruses have a problematic gene expression signature that can be resolved only by viral excision⁵. Another open question is whether standard reprogramming, expansion and directed differentiation processes are robust enough to minimize noise caused by donor-to-donor variation, which could obscure disease-specific phenotypes. Finally, it has not been determined whether individual iPSC lines behave similarly from laboratory to laboratory.

To address these questions and to determine whether cell-line variability might limit the utility of iPSCs, it is necessary to systematically

examine in parallel a sufficiently large set of cell lines. We derived a set of iPSC lines that includes many sources of variation that might be encountered in the course of modeling development or disease, including age, sex, health status and donor identity. We then compared the ability of the lines to undergo directed differentiation as a stringent test of their pluripotency. We selected motor neurons as a model system because they are an example of the many differentiated human cell types that cannot be obtained by other means, and are specifically affected in amyotrophic lateral sclerosis (ALS)¹⁰.

After all cell lines were extensively characterized, we found that, like ESCs, most iPSCs were capable of generating functional motor neurons under a standard differentiation protocol, whereas a few lines required more efficient neuralization. The efficiency with which each individual line generated motor neurons was highly reproducible between two different laboratories, indicating that the collection can function robustly as a shared resource. Potential sources of variation between iPSC lines, such as donor age and transgene expression, did not correlate with differentiation efficiency. Likewise, no significant differences were found between three-factor and four-factor lines, or between lines from healthy and ALS patients. However, we found that two parameters may be associated with differing behavior of lines. Donor identity and donor sex were both associated with variation in

¹The Howard Hughes Medical Institute, Cambridge, Massachusetts, USA. ²Harvard Stem Cell Institute, Department of Stem Cell and Regenerative Biology, Harvard University, Cambridge, Massachusetts, USA. ³Department of Molecular and Cellular Biology, Harvard University, Cambridge, Massachusetts, USA. ⁴Project A.L.S./Jennifer Estess Laboratory for Stem Cell Research, Columbia University, New York, New York, USA. ⁵Departments of Pathology, Neurology and Neuroscience, Columbia University, Center for Motor Neuron Biology and Disease (MNC), and Columbia Stem Cell Initiative (CSCI), New York, New York, USA. ⁶Program in Neurobiology and FM Kirby Neurobiology Center, Children's Hospital Boston, Boston, Massachusetts, USA. ⁷Department of Neurobiology, Harvard Medical School, Boston, Massachusetts, USA. ⁸Department of Anesthesia, Critical Care and Pain Medicine, Massachusetts General Hospital, Boston, Massachusetts, USA. ⁹Departments of Physiology and Cellular Biophysics, and Neuroscience, Columbia University, New York, New York, USA. ¹⁰The New York Stem Cell Foundation, Inc. (NYSCF), New York, New York, USA. ¹¹Present address: iPierian, Inc., South San Francisco, California, USA. ¹²These authors contributed equally to this work. Correspondence should be addressed to K.E. (keggan@scrb.harvard.edu) or H.W. (hw350@columbia.edu).

Table 1 Human stem cell lines used for comparative study

Cell type	Donor fibroblast	Cell line	ALS diagnosis	Reprogramming factors	Sex	Donor age	Reference
iPS	11	11a	Healthy control	OCT4/SOX2/KLF4	M	36	This report
iPS	11	11b	Healthy control	OCT4/SOX2/KLF4	M	36	This report
iPS	11	11c	Healthy control	OCT4/SOX2/KLF4	M	36	This report
iPS	15	15b	Healthy control	OCT4/SOX2/KLF4	F	48	This report
iPS	17	17a	Healthy control	OCT4/SOX2/KLF4	F	71	This report
iPS	17	17b	Healthy control	OCT4/SOX2/KLF4	F	71	This report
iPS	18	18a	Healthy control	OCT4/SOX2/KLF4	F	48	This report
iPS	18	18b	Healthy control	OCT4/SOX2/KLF4	F	48	This report
iPS	18	18c	Healthy control	OCT4/SOX2/KLF4	F	48	This report
iPS	20	20b	Healthy control	OCT4/SOX2/KLF4	M	55	This report
iPS	27	27b	<i>SOD1</i> G85S	OCT4/SOX2/KLF4	F	29	This report
iPS	27	27e	<i>SOD1</i> G85S	OCT4/SOX2/KLF4	F	29	This report
iPS	29	29A	<i>SOD1</i> L144F	OCT4/SOX2/KLF4/ <i>c-MYC</i>	F	82	2
iPS	29	29B	<i>SOD1</i> L144F	OCT4/SOX2/KLF4/ <i>c-MYC</i>	F	82	2
iPS	29	29d	<i>SOD1</i> L144F	OCT4/SOX2/KLF4	F	82	This report
iPS	29	29e	<i>SOD1</i> L144F	OCT4/SOX2/KLF4	F	82	This report
ES	–	HuES-3	–	–	M	–	23
ES	–	HuES-6	–	–	F	–	23
ES	–	HuES-9	–	–	F	–	23
ES	–	HuES-13	–	–	M	–	23
ES	–	HuES-3 hb9:GFP	–	–	M	–	12
ES	–	RUES1	–	–	M	–	24

Sixteen human iPSC lines were used for comparison with each other and with six ESC lines. iPSC lines include 14 newly generated three-factor lines from two ALS patients and five controls, and two previously published four-factor lines from one ALS patient. This cohort of human stem cell lines allows comparisons to be made between ESCs and iPSCs, between three-factor and four-factor iPSC lines, between male and female lines, between lines derived from the same donor and those derived from another donor, and between cells derived from ALS patients and control donors.

differentiation performance and warrant further study. The test set reported here has already served as the basis for an analysis of the epigenetic influences on stem cell differentiation potential¹¹. The test set cell lines are available for distribution and should prove to be a valuable resource for many avenues of stem cell research.

RESULTS

A test set of iPSC lines

We assembled a test set of 16 human iPSC lines, including 14 new lines and 2 previously reported lines² (Table 1). This set comprised lines from seven individuals of both sexes whose ages ranged from 29 to 82 years. All iPSCs were derived by retroviral transduction of skin fibroblasts. Most lines were produced using only three factors (*OCT4*, *KLF4*, *SOX2*) but two lines derived using the additional factor *c-MYC*² were included for comparison. To allow evaluation of the effects of individual genetic background, we included independent lines derived from the same subjects (two lines from each of two donors, three lines from each of two donors and four lines from one donor). Finally, we included lines from both healthy controls (*n* = 10) and patients with ALS (*n* = 6), all of which carried mutations in the superoxide dismutase 1 gene (*SOD1*). To determine whether reprogramming systematically influences stem cell properties, we compared the performance of these iPSC lines to that of six ESC lines (Table 1).

To verify that the newly derived iPSC lines were indeed pluripotent stem cells, we assessed expression of the pluripotency markers alkaline phosphatase, NANOG, *OCT4*, *SSEA3*, *SSEA4*, *TRA-1-60* and *TRA-1-81*. In addition to exhibiting cell-surface staining patterns for both *SSEA* and *TRA-1* proteins, all colonies showed distinct nuclear staining when assayed for NANOG and *OCT4* immunoreactivity (Fig. 1a and Supplementary Fig. 1a). All iPSC lines generated

compact colonies with a morphology (Fig. 1a and Supplementary Fig. 1a) and cell-cycle profile similar to those of ESC controls (Fig. 1b and Supplementary Fig. 1b). We next determined that the test set could differentiate into all three embryonic germ layers as detected by expression of neuron-specific tubulin (*TUJ1*), smooth muscle actin (α SMA) and endodermal α -fetoprotein (*AFP*) after 16 d of differentiation *in vitro* (Fig. 1c and Supplementary Fig. 1c). Lastly, we tested the ability of several lines to generate teratomas in immune-compromised mice. After injection, each line (14/14 tested) formed teratomas containing complex tissue structures characteristic of all three embryonic germ layers (Fig. 1d and Supplementary Fig. 1d). Based on histological criteria these structures included neuronal fibers, hair follicles, melanocytes, keratin pearls, muscle cells, cartilage, glands and goblet cells. Thus our test set resource contains lines that have been extensively characterized and meet the most stringent criteria for pluripotency (Fig. 1e).

Most iPSC lines generate electrically active motor neurons using standard procedures

To rigorously and quantitatively test the potential of iPSCs to undergo terminal differentiation, we determined the efficiency with which each line could generate spinal motor neurons (Fig. 2). In response to standard procedures involving retinoic acid and induction of the sonic hedgehog pathway^{12,13} (Fig. 2a), the majority (19/22) of the iPSC and ESC lines generated cells with a neuronal morphology that expressed *TUJ1* and the motor neuron marker *ISLET 1/2* (*ISL*) (Fig. 2b). To confirm the reliability of the lines as a resource for the community, we transferred the entire test set from the laboratory in which they were derived (Eggen laboratory) to a geographically distinct laboratory (Project A.L.S. (PALS)/Jennifer Estess Laboratory for Stem Cell Research, Columbia University), which then repeated



the directed differentiation experiments. Consistent with the conclusion that the properties of each cell line are reproducible, the same lines were found to generate ISL⁺ neurons (Fig. 2c). Indeed, the differentiation efficiency for each line (ranging from 4–15% ISL⁺/total nuclei) showed no difference between the two laboratories (Fig. 2c; ANOVA $f = 1.132$, $P = 0.301$, Supplementary Table 1). Thus, the test set will also serve as a robust resource for research in other centers.

To confirm that the ISL⁺ neurons were motor neurons, we quantified the expression of other markers indicative of this neural subtype. We found that the iPSC lines producing the highest percentage of ISL⁺ neurons also produced the highest percentage of cells expressing the motor neuron-specific transcription factor HB9 (ref. 14; Fig. 2d). On average, iPSC lines generated HB9⁺ neurons as efficiently as did the established ESC line HuES-13 (Fig. 2h). In addition, in a tested subset of lines, ISL⁺ neurons were immunopositive for ChAT, the enzyme required for acetylcholine synthesis (Fig. 2e). These differentiated cultures, which also contained a variety of motor neuron progenitors, expressed the neural marker NCAM (Supplementary Fig. 2a), and expressed substantial levels of mRNA encoding the markers HB9, ChAT and CHT1 (Supplementary Fig. 2b). Finally, unlike PAX6⁺ progenitors in these cultures, ISL⁺ neurons were never observed to be actively cycling as measured by Ki67 immunostaining (Supplementary Fig. 2c). Although there were quantitative differences in motor neuron generation among the lines (Fig. 2i and Supplementary Table 2), they did not reflect overall differences between iPSC and ESC lines (Fig. 2g and Supplementary Table 1) or between healthy control and ALS iPSC lines

(Fig. 2f and Supplementary Table 1). Moreover, four-factor lines did not underperform relative to three-factor lines (Supplementary Table 1). Therefore, most (13/16) iPSC lines in the resource could generate spinal motor neurons with a reproducible efficiency that is equivalent to that of gold standard ESC lines.

To demonstrate that the motor neurons we produced were functional, we compared the electrophysiological properties of motor neurons from four iPSC lines with motor neurons from two ESC lines (Fig. 3). We first monitored intracellular Ca²⁺ dynamics using the Ca²⁺-sensitive dyes Fura Red AM (Fig. 3a–b) and Fluo-4 AM (Fig. 3c,h,j) to monitor spontaneous activity, and after application of either kainate to activate ionotropic glutamate receptors, or KCl to depolarize the membrane and open voltage-gated Ca²⁺ channels (Fig. 3d–g,i,k). Spontaneous calcium transients were visible in the cell

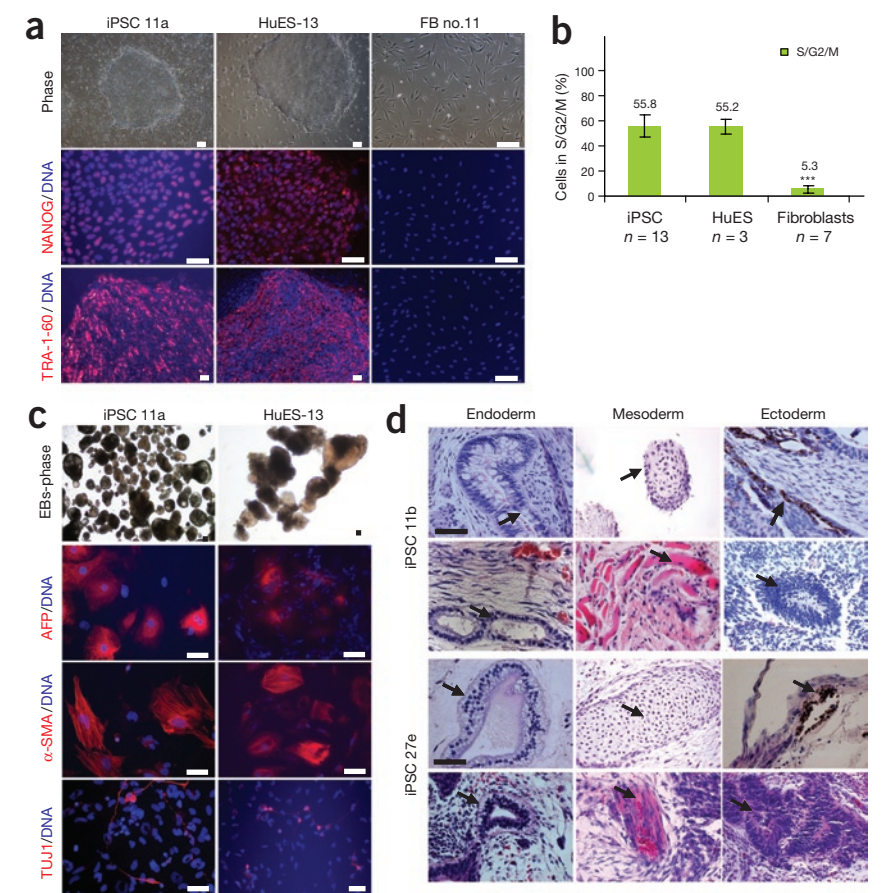
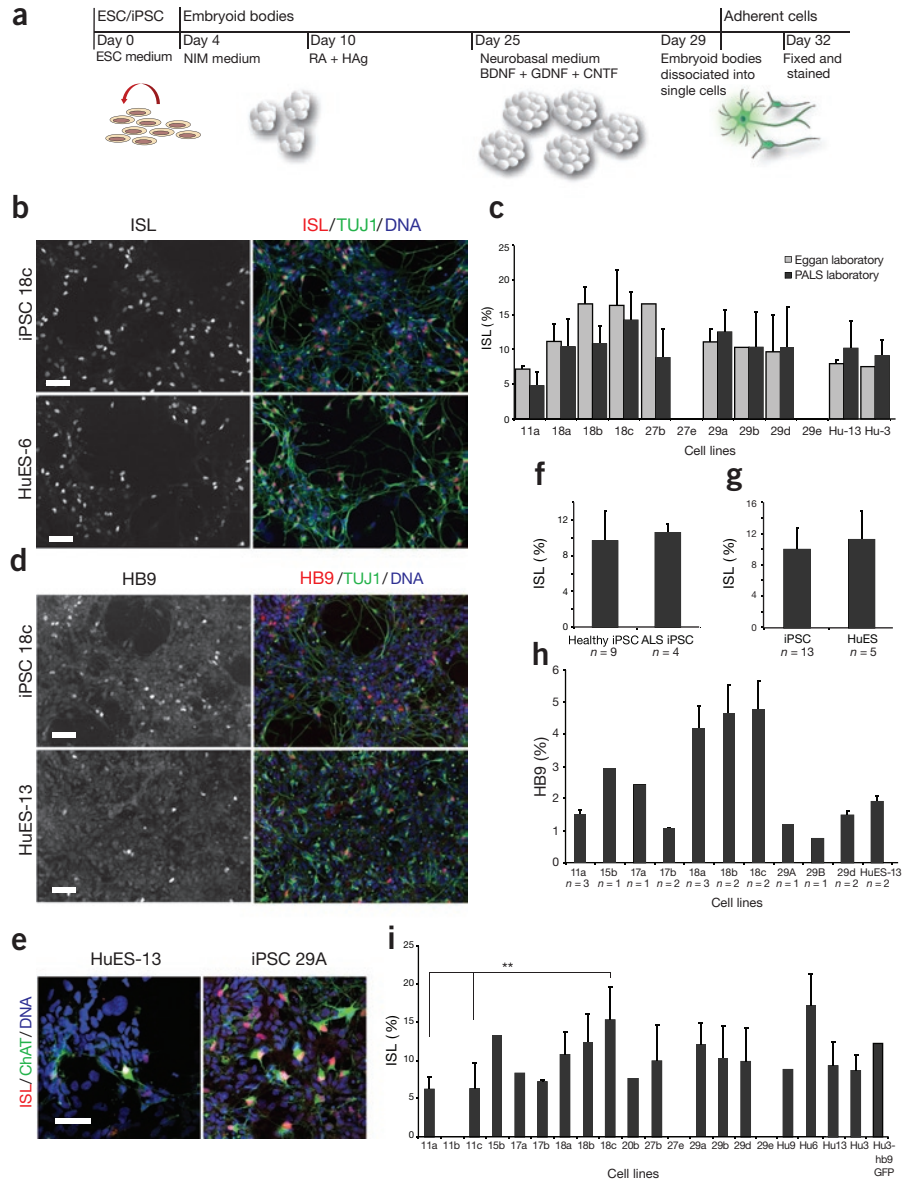


Figure 1 Characterization of pluripotency in the test set of iPSC lines. (a) iPSC colonies were morphologically identical to ESC colonies and expressed the pluripotency markers NANOG and TRA-1-60, unlike the patient fibroblasts from which they were derived. FB, fibroblasts. Scale bars, 200 μ m. (b) iPSC lines showed cell cycle profiles similar to those of ESCs and different from their parental fibroblasts. The percentage of cells at different stages of the cell cycle was determined by propidium iodide staining and flow cytometry. The percentage of cells in S, G2 and M phase was determined for each cell line and then averaged for each category. *** $P < 0.001$, mean \pm s.d. (c,d) Like ESCs, iPSC lines generated cell types of all three embryonic germ layers (endoderm, AFP; mesoderm, α -SMA; ectoderm, TUJ1) *in vitro*, as embryoid bodies (c, EBs; scale bars, 100 μ m), and when injected into mouse kidney capsules and allowed to form teratomas *in vivo* (d; scale bars, 50 μ m). Representative images of H&E-stained sections are shown for lines 11b and 27e. Glands and goblet cells (endoderm), cartilage and muscle (mesoderm), pigmented neural epithelium and neural rosettes (ectoderm) are shown in the top and bottom panels, respectively, for both lines. (e) Summary chart depicting assays by which iPSC lines in the test set were characterized. Pluripotency assays for 29A and B were previously published².

	11a	11b	11c	15b	17a	17b	18a	18b	18c	20b	27b	27e	29A	29B	29d	29e
iPS- alkaline phosphatase	+	+	+	+	+	+	+	+	+	+	+	+	+	+	+	+
iPS- NANOG	+	+	+	+	+	+	+	+	+	+	+	+	+	+	+	+
iPS- OCT4	+	+	+	+	+	+	+	+	+	+	+	+	+	+	+	+
iPS- SSEA3	+	+	+	+	+	+	+	+	+	+	+	+	+	+	+	+
iPS- SSEA4	+	+	+	+	+	+	+	+	+	+	+	+	+	+	+	+
iPS- TRA-1-60	+	+	+	+	+	+	+	+	+	+	+	+	+	+	+	+
iPS- TRA-1-81	+	+	+	+	+	+	+	+	+	+	+	+	+	+	+	+
iPS- cell cycle analysis	+	+	-	+	+	+	+	+	+	+	+	+	-	-	+	+
iPS- <i>in vitro</i> three-germ layer assay	+	+	+	+	+	+	+	+	+	+	+	+	+	+	+	+
iPS- teratoma formation	+	+	+	+	+	+	+	+	+	+	+	+	+	+	+	-
iPS- FC analysis	+	+	+	-	-	+	+	+	+	+	+	+	+	+	+	+
iPS- transgene expression	+	+	+	+	+	+	+	+	+	+	+	+	+	+	+	+
iPS- standard neuronal differentiation	+	+	+	+	+	+	+	+	+	+	+	+	+	+	+	+
iPS- differentiation in both labs	+	-	-	-	-	-	+	+	+	+	+	+	+	+	+	+
iPS- neuralizing differentiation	-	+	-	-	-	-	-	-	-	-	-	-	-	-	-	+
Neurons- transgene expression	+	+	-	+	+	+	+	+	+	+	+	+	-	-	-	+
Neurons- calcium imaging	+	-	-	-	-	-	+	-	+	-	+	-	-	-	-	-
Neurons- patch clamp assays	-	-	-	-	-	-	+	-	-	-	+	-	-	-	-	-

Figure 2 iPSCs show similar capacity for directed motor neuron differentiation compared to ESCs. **(a)** Protocol for directed differentiation of human stem cell lines into motor neurons. Cells were differentiated as embryoid bodies from day 0–29 in media formulations containing morphogens, including retinoic acid (RA), a small molecule agonist of the sonic hedgehog pathway (HAG) and neurotrophic factors BDNF, GDNF and CNTF. Embryoid bodies were dissociated and single cells plated for adherent culture on day 29. On day 32 cultures were analyzed. NIM, neural induction medium. **(b)** Representative immunostaining results for iPSC (18c) and ESC (HuES-6) cultures show many ISL⁺ TUJ1⁺ motor neurons (scale bars, 50 μm). **(c)** The percentage of all nuclei that were ISL⁺ was quantified from differentiations performed independently in the Eggen and PALS laboratories. Data sets from lines differentiated in both laboratories are compared here, are highly similar and have reproducible, characteristic percent ISL⁺ efficiencies. 29e and 27e did not differentiate efficiently in either laboratory. Hu-13, HuES-13; Hu-3, HuES-3. **(d)** Efficiency of motor neuron differentiation was also measured by an alternative marker of motor neuron identity, HB9 (scale bars, 50 μm). **(e)** Many ISL⁺ motor neurons were also ChAT⁺, indicating proper maturation toward a cholinergic transmitter phenotype (scale bar, 50 μm). **(f,g)** iPSC lines from control and ALS patients differentiated into ISL⁺ motor neurons with similar efficiencies (f), as did ESCs and iPSCs (g). **(h)** The percentages of HB9⁺ nuclei were compared for a subset of iPSC lines and HuES-13. Although comparisons again suggest donor- or line-specific differences, iPSC lines were overall equally capable of generating HB9⁺ motor neurons as HuES-13 (mean ± s.d.). **(i)** Percent ISL⁺ data from both laboratories were pooled for each iPSC and ESC line, and comparisons between lines showed generally similar performance, with significant differences between iPSC line 18c and iPSC lines 11a and 11c ($P < 0.05$). Hu, HuES.



bodies and processes of multiple cells from each line, even without treatment (Fig. 3c,h,j; Supplementary Fig. 3a and Supplementary Video 1). Upon exposure to kainate, increases in Ca²⁺ levels were observed in 78% of cells with neuronal morphology (n = 132 cells). Many kainate-responsive cells also exhibited Ca²⁺ transients upon exposure to KCl (Fig. 3i,k). Immunostaining confirmed that many of the cells that responded to kainate and KCl in these mixed cultures were ISL⁺ motor neurons (Fig. 3b,i and Supplementary Fig. 3b).

To further demonstrate that iPSC-derived neurons express the repertoire of voltage-gated ion channels characteristic of active neurons, we made electrophysiological recordings using whole-cell patch clamping. All cells with a neuronal morphology, derived from HuES-3 hb9:GFP (n = 9 cells), iPSC line 18a (n = 10 cells) and iPSC line 27b (n = 10 cells), showed fast voltage-activated inward currents followed by slow outward currents, consistent with voltage-activated sodium and potassium currents, respectively (Fig. 3l,m). Inward currents (n = 5/5) were blocked by tetrodotoxin (TTX), an inhibitor of voltage-gated sodium channels (Fig. 3n). In addition, depolarizing

stimuli in current-clamp mode elicited single action potentials in both ESC-derived (n = 2) and iPSC-derived neurons (n = 2), as well as repetitive firing in a neuron derived from iPSC line 18a (Fig. 3o). Therefore, we conclude that both ESC- and iPSC-derived neurons generated from the cell lines in the resource are similarly functional at a physiological level.

Contribution of other variables to differentiation

Although all cell lines were capable of generating motor neurons, we systematically examined some parameters that have been implicated in differentiation efficiency and so would be of interest to potential users of this resource. The majority of iPSC lines (9 out of 15 tested; Supplementary Fig. 4) exhibited genomic stability at both early (p13) and late (p42) passages. The other six lines (29d, 27b, 29e, 11a, 11b, 15b) acquired disparate abnormalities of varying severity at later passages. However, lines that became karyotypically abnormal did not produce motor neurons with a significantly different efficiency compared with normal lines (P = 0.932; Supplementary Table 1).



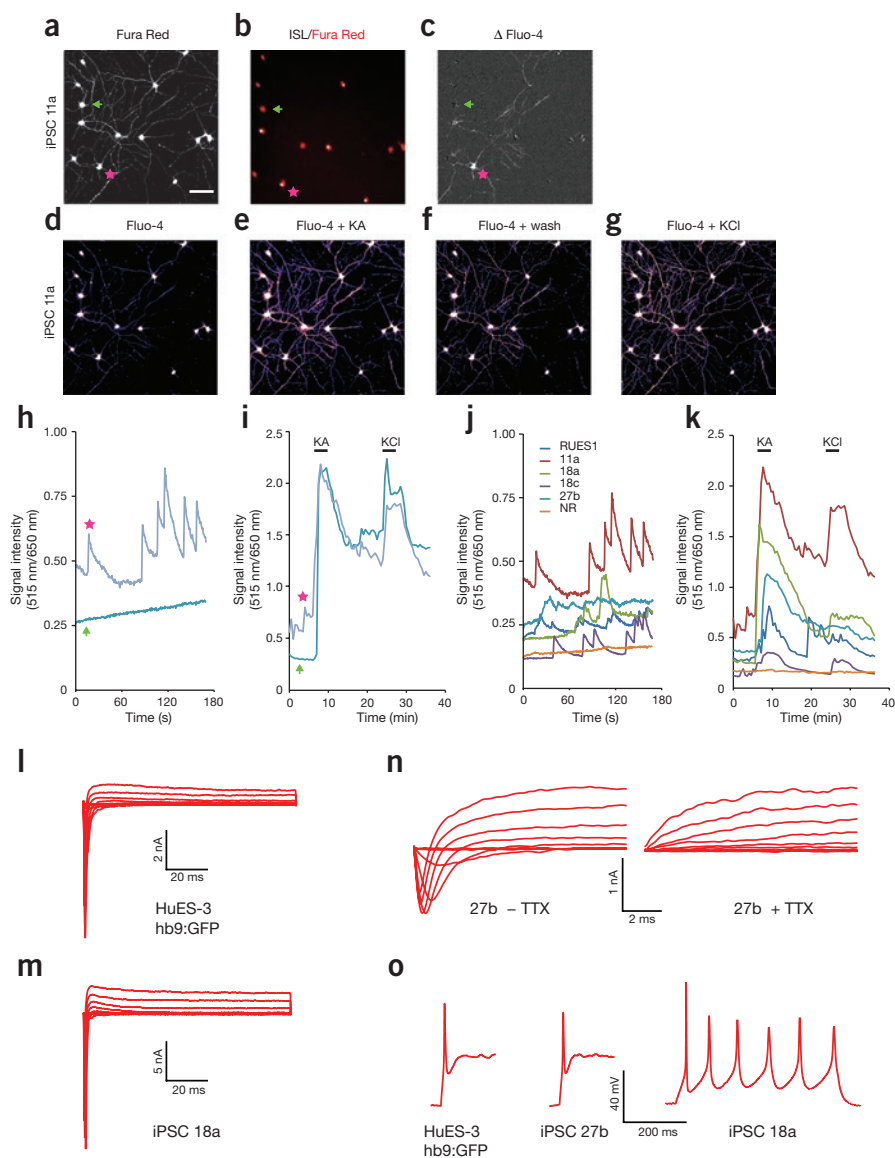
As it is not known how these chromosomal changes may affect the behavior of any given cell type, these lines should be used with caution in studies making phenotypic comparisons.

We and others have reported that reprogramming transgenes can continue to be expressed in patient-specific iPSC lines, but whether they interfere with differentiation has not been fully studied^{2,5}. We therefore used quantitative real time (qRT)-PCR to quantify relative levels of transcription of the reprogramming transgenes from both their endogenous loci and from the integrated retrovirus (Fig. 4a). In most cases, levels of viral transcription were either undetectable or very low compared with levels of transcripts from the endogenous loci; indeed, viral *SOX2* was never detected (Supplementary Fig. 5a). However, a subset of iPSC lines (11b, 11c, 15b, 18b, 18c, 27b, 27e and 29e) continued to express varying levels of viral *KLF4* both in the undifferentiated state and after differentiation to motor neurons (Fig. 4a and Supplementary Fig. 5b–d). Moreover, viral *OCT4* transcripts were present in three of the iPSC lines (15b, 18c and 27b) both before and after differentiation. Notably, there was no correlation between the total level of aggregated transgene expression in iPSCs and the efficiency of motor neuron differentiation as judged

by the percentage of ISL⁺ neurons ($R^2 = 0.1687$). In addition, we carried out immunofluorescence staining for OCT4 and the motor neuron marker ISL (Fig. 4b and Supplementary Fig. 5e). Remarkably, a line such as 15b, which showed persistent transgene expression, generated motor neurons with high abundance, even though many of the motor neurons expressed nuclear OCT4. Therefore, although examples of lines that display karyotypic variation and persistent transgene expression are available in the test set, these phenomena had no detectable effect on rates of motor neuron differentiation.

Finally, we looked at the contribution of age, sex and donor genotype to the outcome of differentiation in our test set. There was no correlation between donor age and the percentage of ISL⁺ neurons generated ($R^2 = 0.0084$). However, there was a significant difference in differentiation efficiency between male and female lines (ANOVA $P = 0.048$, Supplementary Table 3). These sex-specific differences could result from variable processes such as X-chromosome inactivation. Lastly, we compared the ability of independent lines from several of the donors to differentiate into motor neurons. Southern blot analysis (Supplementary Fig. 6a–c) confirmed that lines from donors 11, 18 and 29 arose from distinct reprogramming events. Subsequently,

Figure 3 ESC- and iPSC-derived neurons are physiologically active. (a) Images of iPSC 11a-derived neurons filled with Fura Red AM and Fluo-4 AM dyes. The Fura Red channel is shown. The field illustrated is that imaged in b–g. Activity of labeled cells is represented in h and i. Scale bar, 100 μ m. (b) ISL immunostaining of 11a field in a–g showing ISL⁺ neurons (star) and ISL[−] neurons (arrow). (c) Spontaneous electrical activity in cultured iPSC-derived neurons visualized by a ‘subtracted image’ that shows the difference in pixel intensities between two images acquired 1.7 s apart in the Fluo-4 channel. Higher gray values represent increased pixel intensity. (d–g) Identically exposed pseudocolored averages of ten Fluo-4 AM images taken during the control period before addition of kainic acid (KA) (d), after treatment with 100 μ M KA (e), after washing following KA administration (f) and after treatment with 50 μ M KCl (g). Warmer colors represent increased fluorescence intensity. (h) Plot of Fluo-4/Fura Red intensity ratio in the somata of the two cells indicated by the star and arrow in a–c; only starred cell shows spontaneous activity. (i) Fluo-4/Fura Red intensity ratio of cells in a–c during sequential administration of KA and KCl indicated by bars above graph. (j) Examples of Fluo-4/Fura Red ratios from cell bodies of single spontaneously active cells in cultures of ESC RUES1-derived neurons, and iPSC 11a-, 18a-, 18c- and 27b-derived neurons as well as one example of a nonresponsive (NR), nonactive cell in an RUES1 culture. (k) Response of cells in j to KA and KCl. (l–m) Sample voltage-clamp traces from ESC (l) and iPSC 18a-derived (m) neurons. (n) Blowup of an iPSC 27b-derived neuron recording reveals typical sodium currents (left), which are blocked by 500 nM TTX (right). (o) Current-clamp recordings of single action potentials in ESC and iPSC 27b-derived neurons as well as multiple action potentials in an iPSC 18a-derived neuron.



inspection of the differentiation data (Fig. 2c,h,i) showed that all three iPSC lines from donor 18 produced many motor neurons, whereas the lines from donor 11 performed less well. The difference in differentiation efficiency between line 18c, the best of the three from that donor, and the two lines from donor 11 that generated motor neurons was indeed significant ($P < 0.05$; Fig. 2i; Supplementary Table 2), and when comparisons between averaged differentiation efficiencies of multiple lines from each donor were made, a significant difference was found (ANOVA $P = 0.006$; Supplementary Table 4 and Supplementary Fig. 6d). These results further demonstrate that the cell lines included in the test set may provide an opportunity for other researchers to investigate the effects that sex and other donor-specific phenomenon have in directed differentiation.

Suboptimal lines are rescued by active neuralization

Although the majority of our cell lines reproducibly generated motor neurons, there were three lines (11b, 27e and 29e) that uniformly failed to do so in both laboratories. All three formed embryoid bodies (Fig. 5a, $n = 3-7$ independent experiments per line), but the embryoid bodies from two lines—27e and 29e—became cystic and disaggregated (Fig. 5a). This defect was reflected in a significant decrease in total yield of differentiated cells ($P < 0.05$; Supplementary Fig. 7a and Supplementary Table 5) and by the failure of these two lines to generate TUJ1+ neurons (Supplementary Fig. 7b). A third line—11b—formed embryoid bodies with normal mor-

phology but less than 10% of differentiated cells were TUJ1+ neurons (Fig. 5b). This was significantly lower compared with 18a (Holm-Sidak, $T = 5.037$, $P = 0.002$; Supplementary Table 6), and was in contrast to the results of lines that differentiated appropriately, which produced in excess of 25% TUJ1+ cells (Supplementary Fig. 7b). An indication that early blockade of differentiation might occur in some lines was obtained when we used expression of the antigens SSEA3 and TRA-1-60 to quantify the relative proportion of pluripotent cells within each iPSC line by flow cytometry (Supplementary Fig. 8). One of the recalcitrant iPSC lines (27e) showed higher median fluorescence intensity of TRA-1-60 staining than all others (Supplementary Fig. 8d,e and Supplementary Table 7), suggesting that it might be less prone to spontaneous differentiation.

As the three recalcitrant lines were nevertheless able to initially form embryoid bodies, we tested whether they could be coaxed into the motor neuron differentiation pathway by pushing them toward a more neural fate at the beginning of the differentiation process. We combined our embryoid body protocol with dual SMAD inhibition, similar to a previous report¹⁵, for the first 9 d using SB431542, an inhibitor of transforming growth factor- β 1 activin receptor-like kinase, and LDN193189, a structural analog of the bone morphogenetic protein inhibitor dorsomorphin^{15,16}. Comparing the three underperforming iPSC lines (11b, 27e, 29e) to two ESC lines, we found that the previously defective lines were all neuralized in this optimized protocol and gave rise to the same high abundance of TUJ1+ cells as did the ESC lines (>75%; Fig. 5c,d). Notably, the three iPSC lines that previously could not generate neurons now robustly produced ISL+ (Fig. 5c,e) and HB9+ (Fig. 5f) motor neurons by day 21 at levels indistinguishable from those of both the control ESCs (Fig. 5d-f) and the other 13 iPSC lines (Fig. 2h,i). Thus, although three lines in our human stem cell resource underperformed using a basal differentiation protocol, they could be rescued through a neuralizing protocol to efficiently generate spinal motor neurons.

DISCUSSION

To evaluate iPSCs as a research tool, we generated a large panel of cell lines from multiple donors and examined aspects of the cell lines' pluripotency and ability to generate terminally differentiated motor neurons. The results of our comparisons confirm the remarkable value of iPSC lines for *in vitro* studies and demonstrate that they can perform as well as standard ESC lines. This observation held true for experiments carried out using standardized procedures in two geographically distinct laboratories. The analyses presented here serve as a quality control for this stem cell resource, while also providing sufficient data on specific aspects of variability to allow investigators to select lines of particular relevance to their research.

Our study is not the first to compare human iPSC and ESC lines, but it is the most extensive comparison of their ability to generate a specific terminally differentiated cell thus far. Most studies have used panels of four or fewer iPSC lines¹⁷⁻²², limiting the

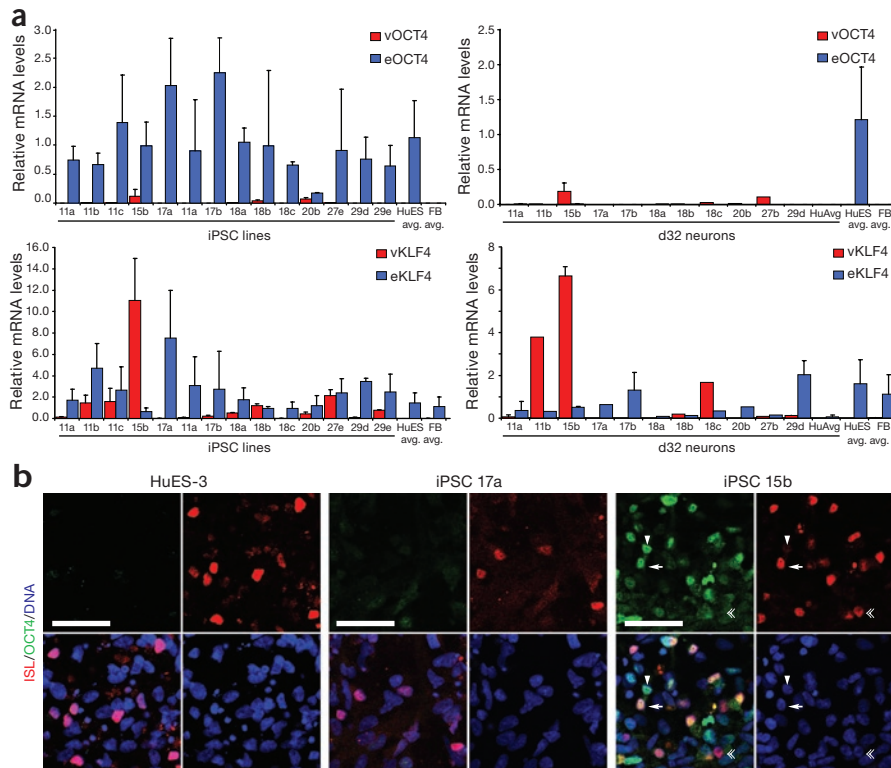


Figure 4 Persistent transgene expression does not inhibit differentiation. (a) qRT-PCR was used to measure relative levels of transcript from endogenous genes 'e' and viral transgenes 'v' of the reprogramming factors *OCT4* and *KLF4* in undifferentiated iPSCs and ESCs, and in day 32 neuron cultures. Transgene expression or silencing in the undifferentiated cells is maintained after differentiation. Relative levels in undifferentiated HuES-3 were set as 1. FB, fibroblasts. (b) Day 32 motor neuron cultures were co-stained for ISL and OCT4. HuES-3- and iPSC 17a-derived cultures, which do not express viral OCT4, did not stain for OCT4. However, iPSC 15b-derived cultures, which do express viral OCT4, contained many OCT4+ ISL+ motor neurons and OCT4+ ISL- cells. Arrow, OCT4+ ISL+; arrowhead, OCT4+ ISL-; chevron, OCT4- ISL+. Scale bars, 50 μ m.



possibilities for understanding variability between cell lines or for drawing general conclusions about functional similarities between iPSCs and ESCs. Similar to a previous report that examined four iPSC lines and one ESC line for generation of terminally differentiated motor neurons⁹, we found that the differentiation efficiencies of individual iPSC lines vary. However, the earlier study showed that the differentiation capacity of iPSCs was inferior to that of ESCs, whereas we found that iPSC lines could be made to differentiate on average as well as ESC lines. Whether the difference in the conclusions of the two studies is due to differences in the protocols for reprogramming and motor neuron differentiation, or whether it reflects differences in the numbers of samples analyzed, remains to be determined.

Although all cell lines in our test set were capable of generating motor neurons, application of the standard protocol for motor neuron production did reveal significant quantitative differences in the propensity of the lines for terminal differentiation. These differences were highly reproducible, suggesting that they represent intrinsic characteristics of the lines. Our initial hypothesis was that the poorly performing lines would be identified by anomalies in standard tests for stem cell quality. However, all cell lines tested expressed pluripotency markers and could form the three germ layers *in vitro* and in teratomas. Moreover, although variations in karyotype and transgene expression were observed, they were not accurate predictors of differentiation capacity. Fortunately, a solution for identifying such predictors has now been proposed by a laboratory that used our test set to search for epigenetic and transcriptional differences that correlate with differentiation potential¹¹. Using the lines we describe here, they developed a scorecard for stem cell quality that predicted our motor neuron differentiation results (Fig. 2i) with remarkable precision.

We anticipate that one of the major uses of the cell lines provided through this resource will be to model ALS. Notably, our data demonstrate that several conditions that are necessary for reliable disease modeling are met. First, because ALS is not a developmental disease, our finding that iPSCs carrying an ALS-triggering mutation differentiated similarly to those from healthy controls is as expected. Second, although lines from different healthy donors, taken together, showed donor-related variation in differentiation efficiency, the pairwise comparisons did not reach significance. This increases the chances that phenotypic differences we may eventually observe between ALS cases and controls are related to disease. Nevertheless, as we found real line-to-line differences, it will be essential to confirm that any phenotypes are ALS-related by silencing the mutant *SOD1*. Lastly, the strong concordance between the results from two different laboratories reported here suggests

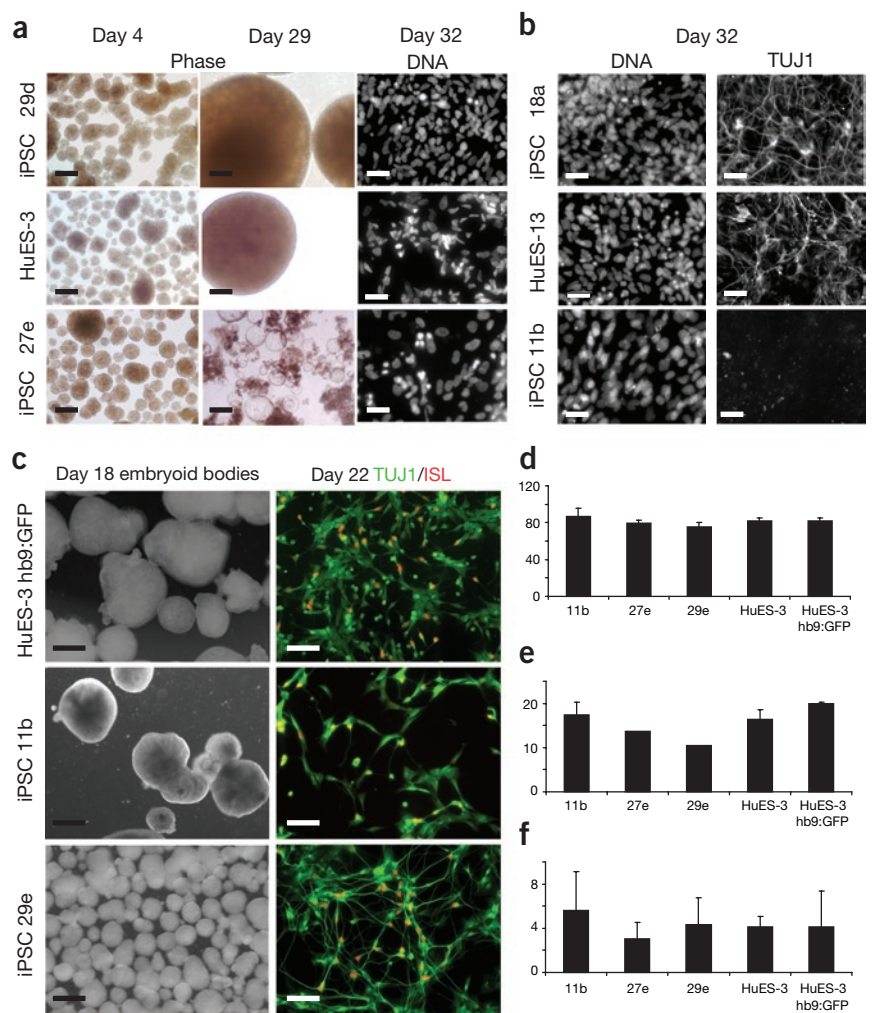


Figure 5 Suboptimal iPSC lines can be rescued using SMAD inhibition. (a) During standard differentiation, iPSC lines 27e and 29e showed abnormal embryoid body morphology and survival compared to lines that behaved normally (HuES-3 and 29d shown); phase scale bar, 500 μ m; DNA scale bar, 129 μ m. (b) Although embryoid bodies from iPSC line 11b had typical morphology, day 32 cultures showed decreased neuronal TUJ1 staining compared to all other normal lines (HuES-13 and iPSC 18a shown), scale bar, 129 μ m. (c) Representative phase and immunostaining images for previously defective iPSC lines 29e, 11b, and control ESC lines HuES-3 and HuES-3-hb9:GFP. Phase image scale bars are 500 μ m, immunostaining image scale bars are 100 μ m. (d–f) Quantification of immunostaining in differentiated cultures derived from the three previously problematic iPSC lines (11b, 27e, 29e) and ESC controls; percentage of TUJ1+ cells (d); percentage of ISL+ cells (e); and percentage of HB9+ cells (f). Mean \pm s.e.m.

that, once ALS-related phenotypic differences are discovered, they will prove sufficiently reproducible to serve as a foundation for research on ALS.

METHODS

Methods and any associated references are available in the online version of the paper at <http://www.nature.com/naturebiotechnology/>.

Note: Supplementary information is available on the Nature Biotechnology website.

ACKNOWLEDGMENTS

We thank H. Mitsumoto, J. Montes, P. Kaufmann and J. Andrews for collecting skin biopsies; K. Koszka, A. Sproul, A. Hon and A. Garcia-Diaz for technical assistance; M. Park, A. Meissner and C. Bock for manuscript assistance, as well as S. Brenner-Morton and T. Jessell for providing Islet antibodies. This work was

funded by Project A.L.S., NYSYSTEM and the National Institutes of Health (NIH) GO grant 1RC2 NS069395-01. G.L.B. is a Harvard Stem Cell Institute/NIH Trainee. E.K. is an EMBO Postdoctoral Fellow. B.J.W. is supported by NIH Training Grant 5T32GM007592. C.J.W. is supported by grants from the National Institute of Neurological Disorders and Stroke and the National Institute of Child Health and Development. K.E. is a Howard Hughes Medical Institute early career scientist.

AUTHOR CONTRIBUTIONS

G.F.C., M.W.A. and D.H.O. maintained human fibroblasts. C.T.R. and J.T.D. reprogrammed all iPSC lines. G.L.B. and E.K. expanded all iPSC lines. G.L.B. and E.K. led and contributed equally to all other experiments and analyses in the Eggen laboratory. G.F.C., M.W.A. and D.H.O. led and contributed equally to all other experiments and analyses in the Project ALS laboratory. D.J.K. did FC analysis. A.B.M., D.J.W. and D.H.O. designed and carried out Ca²⁺ imaging. B.J.W., G.L.B. and C.J.W. did recordings. M.Y. assisted with teratomas. L.D. assisted with quantitative analysis. S.M. assisted with stem cell culture. G.L.B., E.K., K.E., G.F.C., M.W.A., D.H.O., C.E.H. and H.W. conceived the experiments and wrote the manuscript.

COMPETING FINANCIAL INTERESTS

The authors declare no competing financial interests.

Published online at <http://www.nature.com/naturebiotechnology/>.
Reprints and permissions information is available online at <http://npg.nature.com/reprintsandpermissions/>.

1. Kiskinis, E. & Eggen, K. Progress toward the clinical application of patient-specific pluripotent stem cells. *J. Clin. Invest.* **120**, 51–59 (2010).
2. Dimos, J.T. *et al.* Induced pluripotent stem cells generated from patients with ALS can be differentiated into motor neurons. *Science* **321**, 1218–1221 (2008).
3. Park, I.H. *et al.* Disease-specific induced pluripotent stem cells. *Cell* **134**, 877–886 (2008).
4. Lee, G. *et al.* Modelling pathogenesis and treatment of familial dysautonomia using patient-specific iPSCs. *Nature* **461**, 402–406 (2009).
5. Soldner, F. *et al.* Parkinson's disease patient-derived induced pluripotent stem cells free of viral reprogramming factors. *Cell* **136**, 964–977 (2009).
6. Chin, M.H. *et al.* Induced pluripotent stem cells and embryonic stem cells are distinguished by gene expression signatures. *Cell Stem Cell* **5**, 111–123 (2009).
7. Doi, A. *et al.* Differential methylation of tissue- and cancer-specific CpG island shores distinguishes human induced pluripotent stem cells, embryonic stem cells and fibroblasts. *Nat. Genet.* **41**, 1350–1353 (2009).
8. Stadtfeld, M. *et al.* Aberrant silencing of imprinted genes on chromosome 12qF1 in mouse induced pluripotent stem cells. *Nature* **465**, 175–181 (2010).
9. Hu, B.Y. *et al.* Neural differentiation of human induced pluripotent stem cells follows developmental principles but with variable potency. *Proc. Natl. Acad. Sci. USA* **107**, 4335–4340 (2010).
10. Kanning, K.C., Kaplan, A. & Henderson, C.E. Motor neuron diversity in development and disease. *Annu. Rev. Neurosci.* **33**, 409–440 (2010).
11. Bock, C. *et al.* Reference maps of human ES and iPSC cell variation enable high-throughput characterization of pluripotent cell lines. *Cell* published online, doi:10.1016/j.cell.2010.12.032 (3 February 2011).
12. Di Giorgio, F.P., Boulting, G.L., Bobrowicz, S. & Eggen, K.C. Human embryonic stem cell-derived motor neurons are sensitive to the toxic effect of glial cells carrying an ALS-causing mutation. *Cell Stem Cell* **3**, 637–648 (2008).
13. Wichterle, H., Lieberam, I., Porter, J.A. & Jessell, T.M. Directed differentiation of embryonic stem cells into motor neurons. *Cell* **110**, 385–397 (2002).
14. Arber, S. *et al.* Requirement for the homeobox gene Hb9 in the consolidation of motor neuron identity. *Neuron* **23**, 659–674 (1999).
15. Chambers, S.M. *et al.* Highly efficient neural conversion of human ES and iPSC cells by dual inhibition of SMAD signaling. *Nat. Biotechnol.* **27**, 275–280 (2009).
16. Zhou, J. *et al.* High-efficiency induction of neural conversion in human ESCs and human induced pluripotent stem cells with a single chemical inhibitor of transforming growth factor beta superfamily receptors. *Stem Cells* **28**, 1741–1750 (2010).
17. Taura, D. *et al.* Adipogenic differentiation of human induced pluripotent stem cells: comparison with that of human embryonic stem cells. *FEBS Lett.* **583**, 1029–1033 (2009).
18. Tokumoto, Y., Ogawa, S., Nagamune, T. & Miyake, J. Comparison of efficiency of terminal differentiation of oligodendrocytes from induced pluripotent stem cells versus embryonic stem cells in vitro. *J. Biosci. Bioeng.* **109**, 622–628 (2010).
19. Xi, J. *et al.* Comparison of contractile behavior of native murine ventricular tissue and cardiomyocytes derived from embryonic or induced pluripotent stem cells. *FASEB J.* **24**, 2739–2751 (2010).
20. Armstrong, L. *et al.* Human induced pluripotent stem cell lines show stress defense mechanisms and mitochondrial regulation similar to those of human embryonic stem cells. *Stem Cells* **28**, 661–673 (2010).
21. Ghosh, Z. *et al.* Persistent donor cell gene expression among human induced pluripotent stem cells contributes to differences with human embryonic stem cells. *PLoS ONE* **5**, e8975 (2010).
22. Grigoriadis, A.E. *et al.* Directed differentiation of hematopoietic precursors and functional osteoclasts from human ES and iPSC cells. *Blood* **115**, 2769–2776 (2010).
23. Cowan, C.A. *et al.* Derivation of embryonic stem-cell lines from human blastocysts. *N. Engl. J. Med.* **350**, 1353–1356 (2004).
24. James, D., Noggle, S.A., Swigut, T. & Brivanlou, A.H. Contribution of human embryonic stem cells to mouse blastocysts. *Dev. Biol.* **295**, 90–102 (2006).



ONLINE METHODS

Cells and cell culture. All cell cultures were maintained at 37 °C, 5% CO₂. Human fibroblasts were cultured in KO-DMEM (Invitrogen), supplemented with 20% Earl's salts 199 (Gibco) and 10% hyclone (Gibco), 1× GlutaMax, penicillin/streptomycin (Invitrogen) and 100 μM 2-mercaptoethanol (Gibco). HuES and iPSCs were maintained on gelatinized tissue culture plastic on a monolayer of irradiated CF-1 mouse embryonic fibroblasts (MEFs) (GlobalStem), in hES media²³, with substitution of plasmanate (Talecris) by an additional 10% knockout serum replacement (Invitrogen) in PALS laboratory only supplemented with 20 ng/ml of bFGF. Media was changed every 24 h and lines were passaged by trypsinization (0.5% trypsin EDTA, Invitrogen) or dispase (Gibco, 1 mg/ml in hES media for 30 min at 37 °C).

Derivation of human fibroblasts and iPSC generation. Human fibroblasts were generated from 3 mm forearm dermal biopsies after informed consent was obtained, as reported previously². The murine leukemia retroviral vector pMXs containing the human cDNAs for *KLF4*, *SOX2* and *OCT4* (ref. 2) were modified to produce higher titer virus by including the Woodchuck Post-transcriptional Responsive Element (WPRES) of FUGW (Addgene plasmid 14883) downstream of the cDNA. Vesicular stomatitis virus (VSV)-g pseudotyped viruses were packaged and concentrated by the Harvard Gene Therapy Initiative at Harvard Medical School. To produce iPSCs, 30,000 human fibroblasts were transduced at a multiplicity of infection of 10–15 with viruses containing all three genes in hES medium with 8 μg/ml polybrene (Sigma-Aldrich). Cells were incubated with virus for 24 h before medium was changed to standard fibroblast medium for 48 h. Cells were subsequently cultured in standard hES medium and iPSC colonies were manually picked based on morphology within 2–4 weeks.

Southern blot analysis. Genomic DNA was extracted from day 21 or day 29 motor neuron differentiation samples for each line using QIAamp DNA Mini kit (Qiagen) according to manufacturer's protocols, including RNase digestion. 8 μg gDNA was restricted with BglII overnight according to standard protocols and 6.5 μg run on a 0.8% agarose gel. Neutral Southern capillary transfer was performed overnight, using Amersham Ny⁺ membrane. OCT4 and SOX2 probes were generated by PCR amplification from *OCT4* and *SOX2* cDNA plasmids² using the following primers (*OCT4* primer forward: GAGAAGGAGAAGCTGGAGCA, reverse: GTGAAGTGAGGGCTCCCAT, 620 bp product; *SOX2*, primer forward: AGAACCCCAAGATGCACAAC, reverse: TGGAGTGGGAGGGAAGAGGTA, 600 bp product) and Roche PCR DIG Probe Synthesis Kit following manufacturer's instructions. DNA was bound to membrane by UV, then probe was hybridized overnight (45 °C for *OCT4*, 55 °C *SOX2*) using DIG Easy Hyb, followed by immunolabeling with anti-digoxigenin-alkaline phosphatase Fab fragments and detection with CPD-Star chemiluminescent substrate (Roche, following manufacturer's protocols). After hybridization with *OCT4* probe, the blot was stripped in 0.4 M NaOH, 0.1% SDS for 40 min at 65 °C, then washed twice in 2× SSC (Fisher) at 25 °C for 15 min, and reprobed with *SOX2* specific probe. Blots were imaged on a KODAK Image Station 4000MM Pro.

Flow cytometry for TRA-1-60, SSEA3 and NCAM. Trypsinized suspensions of ~1 M single cells, at day 0 or day 29 of differentiation, were fixed in 4% PFA for 30 min at 4 °C. After washing in PBS, cell suspensions were incubated with the following antibodies obtained from BD Biosciences: SSEA3 PE (1:100, 560237), Tra-1-60 AlexaFluor647 (1:100, 560219) or the neural differentiation marker NCAM (CD56 V450 BD biosciences 1:100, 560361) for 30 min protected from light at 4 °C. Stained cells were washed once with PBS and analyzed immediately thereafter on a 5 laser ARIA-IIu ROU Cell Sorter configured with a 100 mm ceramic nozzle and operating at 20 p.s.i. SSEA3⁺Tra-1-60⁺ populations were analyzed first by forward and side-scatter properties (FSC, SSC) then analysis gates were set using a combination of fluorescence minus one (FMO) and isotype controls.

Cell cycle analysis. Fibroblasts, ESCs and iPSCs were trypsinized to single cells, fixed overnight in cold 70% ethanol, treated with RNaseA (Qiagen) and stained with propidium iodide (PI; 50 μg/ml, Invitrogen) in 0.1% BSA for at least 30 min. Cells were analyzed using the BD Biosystem LSRII FACS analyzer by doublet discrimination, giving rise to a histogram of PI signal with clear 2n and 4n peaks.

Spontaneous *in vitro* three-germ layer differentiation. Whole stem cell colonies were isolated by dispase treatment and plated in suspension in low-cluster 6-well

plates (Corning) in hES media without bFGF and plasmanate. Cells aggregated to form embryoid bodies within 24 h. Media was replaced every 48 h, and on day 16 embryoid bodies were trypsin and/or mechanically dissociated and plated on gelatin-coated tissue culture plastic for another 2–7 d of adherent culture before fixation and staining.

Teratoma assay. iPSC lines were trypsinized to single cells, washed and resuspended in a minimal volume of CMF-PBS (Cellgro), supplemented with 10% FCS (Invitrogen). At least 1 × 10⁶ cells were injected into the left kidneys of 5- to 6-week-old, severe combined immunodeficient hairless outbred (SHO) mice (3–5 mice/cell line). Xenograft tissue masses formed within 62–131 d, which were extracted, fixed, paraffin-embedded, sectioned and H&E stained. Cells representing all three germ layers were identified after careful examination under the microscope. Further staining images and individual cell line details available upon request.

qRT-PCR. Total RNA was isolated using Trizol LS (Invitrogen), 1 μg was treated with DNase (Invitrogen) and was subsequently used to synthesize cDNA with iScript (Bio-Rad). qRT-PCR was then performed using SYBR green (Bio-Rad) and the iCycler system (Bio-Rad). Quantitative levels for all genes were normalized to endogenous GAPDH. For pluripotency genes, levels were expressed relative to the levels in human ES line HuES-3, for motor neuron genes, levels are expressed relative to human ES line HuES-3 hb9-GFP. Standard curves were run to ensure equal efficiency of all primers, and RNA from 293 cells transfected with the plasmids encoding the transgenes was used as a positive control for viral transgene detection. Primer sequences are available upon request.

Immunocytochemistry. Pluripotency marker, three-germ layer and OCT3/4–ISL1 stains were applied after fixation overnight in 4% paraformaldehyde at 4 °C, as previously described². Neuronal cultures were fixed in 4% PFA for 15–30 min at 4 °C, permeabilized and quenched with 0.1–0.2% Triton-X in PBS (wash buffer) and 100 mM glycine (Sigma) for 20 min. Cells were blocked in wash with 10% donkey serum for 30 min and then incubated in primary antibody overnight, secondary antibodies for 1 h. Primary antibodies used in this study are SSEA-3 (1:2, Developmental Studies Hybridoma Bank (DSHB)), SSEA-4 (1:2, DSHB), TRA1-60 (1:500, Chemicon), TRA1-81 (1:500, Chemicon), NANOG (1:500, R&D), OCT3/4 (1:500, Santa Cruz), AFP (1:500, DAKO), α-SMA (1:500, Sigma), ISL (1:200, DSHB, 40.2D6 or 39.4D5, both of which detect Islet1 and Islet2 in the identical pattern *in vivo* in mouse and chick, Susan Morton, personal communication), HB9 (1:100, DSHB), ChAT (1:100, Chemicon), TUJ1 (1:1,000, Sigma), Ki67 (1:400, Abcam), and Pax6 (1:50, DSHB). Alkaline phosphatase activity was detected in live cultures using the alkaline phosphatase substrate kit (Vector) according to the manufacturer's instructions. Secondary antibodies used in the Eggen laboratory were AlexaFluor 488, 555, 594 and 647 conjugated (1:300, Invitrogen) and images were acquired on the Opera High-Content Screening System (PerkinElmer) for ISL and HB9 quantifications, and otherwise using an Olympus IX51 epi-fluorescence microscope, or an LSM 510 META confocal microscope (Zeiss). Secondary antibodies used in the PALS laboratory were DyLight 488, 549, 647 conjugated (1:1,000, Jackson ImmunoResearch) and images (9, 10× fields/sample) were acquired on a fully automated Zeiss Observer Z1 epi-fluorescence microscope.

Motor neuron differentiation. Pluripotent stem cell colonies were treated with dispase (1 mg/ml) to separate colonies from feeder cells, then with 10 μM ROCK inhibitor Y-27632 (Sigma) for 1 h in suspension, then followed by trypsinization to single cells, and seeded in low-adherence dishes at 0.2–0.4 million cells/ml in hES medium with 20 ng/ml of bFGF and 10 μM Y-27632 for the first 3 d. At day 4 embryoid bodies were switched to a neural induction medium (DMEM/F12 with L-glutamine, NEAA, penicillin/streptomycin, heparin (2 μg/ml), N2 supplement (Invitrogen) and bFGF (20 ng/ml). At day 10, retinoic acid (RA) (0.1 μM, Sigma), ascorbic acid (0.4 μg/ml, Sigma), db-cAMP (1 μM, Sigma) and 0.1 μM HAG were added. At day 17 the concentration of HAG was increased to 1 μM. At day 25 the base medium was changed to Neurobasal (Invitrogen), with all previous factors and with the addition of 10 ng/ml each of BDNF, GDNF and CNTF (R&D). At day 29 embryoid bodies were dissociated with 0.05% trypsin (Invitrogen), and plated onto poly-D-lysine laminin-coated chamber slides (BD Biosciences) at 0.2–0.5 million cells/well. Plated neuron cultures were cultured in the same medium

with the addition of B27 (Invitrogen), 25 μM β -mercaptoethanol (Millipore) and 25 μM glutamic acid (Sigma), and fixed 3 d later.

Neuralizing motor neuron differentiation. iPSCs and ESCs were differentiated as described above, but with the following modifications: differentiations were started from dispased colonies triturated to become \sim 50-cell aggregates of iPSCs, and from days 1–9 were cultured in the presence of SB431542 (10 μM , Sigma-Aldrich) and LDN193189 (0.2 μM , Stemgent) to neuralize the cultures. From day 5 onward, BDNF (10 ng/ml, R&D), ascorbic acid (0.4 $\mu\text{g}/\text{ml}$, Sigma) and RA (Sigma) were added. From day 7 onward, Smoothened agonist 1.3 (SAG) (Calbiochem) was added at 0.5 μM to replace HAG. Aggregates were dissociated, plated and assayed as described above on day 21.

Quantitative image analysis. Quantitative image analysis of differentiated neuronal cultures, for DAPI, TUJ1, ISLET and HB9, was done using the multi-wavelength cell scoring module in MetaMorph (Molecular Devices) software by the PALS laboratory, or Opera/Acapella software (PerkinElmer) by the Eggen laboratory. In brief, intensity thresholds were set, blinded to sample identity, to selectively identify as positive cells, which displayed unambiguous signal intensity above local background. These parameters were used on all samples, and only minimally adjusted for different staining batches as necessary. Script and Parameter files available upon request. Eggen: a minimum of 20,000–160,000 cells per sample were analyzed from 60–180 $20\times$ fields per sample. PALS: a minimum of 4,000 cells per sample were analyzed from nine $10\times$ fields per sample.

Total cell number analysis. As different image field sizes were used in different laboratories, total cells/field were normalized as follows. For all cell lines differentiated in parallel in both laboratories, the mean value for each line was averaged with the mean value of the other lines in this set. These values then generated a ratio (mean cells/field in PALS laboratory/mean cells/field in Eggen laboratory), which was then used to normalize the values from the Eggen laboratory to those from the PALS laboratory.

Voltage-clamp and current-clamp recordings. Differentiated d44 embryoid bodies were dissociated, plated at 8,000 cells/ cm^2 on lysine/laminin-coated coverslips, and allowed to mature for 6 d. Whole-cell voltage-clamp or current-clamp recordings were made using a Multiclamp 700B (Molecular Devices) at 21–23 $^{\circ}\text{C}$. Data were digitized with a Digidata 1440A A/D interface, and recorded and analyzed using pCLAMP 10 software (Molecular Devices). Data were sampled at 20 kHz and low-pass filtered at 2 kHz. Patch pipettes were pulled from borosilicate glass capillaries on a Sutter Instruments P-97 puller and had resistances of 2–4 M Ω . The pipette capacitance was reduced by wrapping the shank with Parafilm

and compensated for using the amplifier circuitry. Series resistance was typically 5–10 M Ω , always <15 M Ω , and compensated by at least 80%. Linear leakage currents were digitally subtracted using a P/4 protocol. Leak currents were typically <100 pA, but occasionally leak currents up to 500 pA were tolerated to accurately document the percentage of cells with voltage-activated sodium currents. Voltages were elicited from a holding potential of -90 mV to test potentials ranging from -90 mV to 20 mV in 10 mV increments. The intracellular solution was a potassium-based solution and contained (mM) KCl, 135; MgCl₂, 2; HEPES, 10 (pH 7.4 with KOH). The extracellular was sodium-based and contained NaCl, 135; KCl, 5; CaCl₂, 2; MgCl₂, 1; glucose, 10; HEPES, 10, pH 7.4 with NaOH). Tetrodotoxin was purchased from Tocris Bioscience.

Ca²⁺ imaging. ES and iPSCs were differentiated under the neuralizing motor neuron differentiation protocol above, dissociated at day 21, cryopreserved, seeded on 15–25 mm diameter coverslips at a density of 125,000–250,000 cells per coverslip in standard media, and matured 12–14 d before Ca²⁺ imaging. Cells were loaded with 5 μM Fura Red AM and 3 μM Fluo-4 AM (Invitrogen) dissolved in 0.2% dimethyl sulfoxide/0.04% pluronic acid (Sigma-Aldrich) in HEPES-buffered physiological salt solution (PSS) for 1 h at 25 $^{\circ}\text{C}$. PSS contained (mM): NaCl 145, KCl 5, HEPES 10, CaCl₂ 2, MgCl₂ 2 and glucose 5.5, pH 7.4. Cultures were continuously superfused with PSS at a rate of \sim 0.5 ml/minute. The cultures were imaged on a C-1 inverted confocal microscope (Nikon Instruments). The fluorescent Ca²⁺ indicators were excited using a 488 nm solid-state laser and emitted light from the Fluo-4 and Fura-Red recorded in separate channels using 500–530 nm band-pass and 650 nm long-pass filters, respectively. We acquired 256 \times 256 pixel images using a 20 \times 0.7 NA air objective (Nikon). For imaging spontaneous Ca²⁺ transients, single sets of 300 images were acquired at a rate of \sim 2 Hz from each coverslip. For the kainate and KCl experiments, 36 images were acquired at a rate of 0.033 Hz and the superfusing PSS was replaced with PSS containing kainate (100 μM) or KCl (50 mM). The NaCl concentration of the PSS was reduced to maintain a constant osmolality and Cl⁻ concentration. Image analysis was performed using ImageJ (<http://rsb.info.nih.gov/ij/>) and custom-written macros. Ca²⁺ transients were determined from regions of interest encompassing the soma of individual cells, using the ratio of intensities from the Fluo-4 and Fura Red channels. Two cultures obtained from a single differentiation of each cell line were used for the kainate and KCl Ca²⁺ imaging experiments.

Statistical analyses. All quantitative data were analyzed using SigmaPlot. Sample groups were subject to One Way ANOVA, with Holm-Sidak *post hoc* pairwise comparisons, or, if equal variance tests failed, by Kruskal-Wallis ANOVA on ranks, with Dunn's *post hoc* pairwise comparisons. Alpha was set at 0.05 for all ANOVAs, ANOVAs on ranks and *post hoc* tests.